

SAUD - 98 - 8450C

M98050609

CONF-9710153--

Mechanical Properties of S-65C Grade Beryllium at Elevated Temperatures

S. H. Goods^a and D. E Dombrowski^b

^aSandia National Laboratories¹
Livermore, CA, USA 94550

^bBrush-Wellman Inc.
Cleveland, OH, USA 44110

RECEIVED

NOV 24 1997

OSTI

Tensile property measurements and fractographic analysis of S-65C beryllium are reviewed. Tests were performed on specimens oriented in the longitudinal and transverse directions with respect to the direction of vacuum hot-pressing. Specimens were tested in air at RT, 100°C, 200°C, 300°C, 415°C and 500°C at an initial strain rate of $1.1 \times 10^{-4} \text{ sec}^{-1}$. Ductility of the material was strongly affected by the test temperature, exhibiting a peak ductility at 300°C. The material displayed a yield point phenomenon which was most pronounced at this same temperature. Scanning electron microscopy was performed on the resulting fracture surfaces and observations are reported.

1. INTRODUCTION

Mechanical properties of beryllium are sensitive to a variety of factors including impurity content and test temperature. Here we report the results of a study in which the tensile properties of grade S-65C beryllium were measured at temperatures between 25°C and 500°C. This grade is produced via vacuum hot pressing of Be powder according to standard powder metallurgy processes. The S-65C grade is of higher purity than other commercial Be grades (S-200F, for example), particularly with respect to BeO and Al.

Borch states that the decrease in beryllium elongation at elevated temperatures is due to the formation of low melting point grain boundary phases [1]. S-65C differs from other commercial beryllium grades in that it has a lower total amount of metallic impurities (including Al), has a closely controlled Fe/Al ratio, and undergoes a special heat treatment to maximize conversion of all aluminum impurities from low melting point metallic aluminum to the higher melting point intermetallic compound AlFeBe_4 .

1.1 Alloy processing

Processing of the S-65C begins with vacuum cast ingots that are about 0.9 m in length and 0.4 meters in diameter. These ingots are then cut into large flat chips using an engine lathe with a seventeen tool cutter. The chips are ground into powder to achieve a fine grain size (7 - 11 μm).

Anisotropy is minimized by randomizing the orientation of the basal plane. This is done by impact grinding the chips into smaller and more isotropic particles. Impact grinding yields minus 325 mesh powder particles which have a cube-like morphology. The impact ground powder is subsequently vacuum hot pressed in cylindrical dies at 1050 - 1150°C and at a pressure of about 7 MPa. Duration of pressing depends on the size of billet. Vacuum hot pressing of the impact ground powder yields good mechanical properties with much reduced anisotropic mechanical behavior compared to the previous grade made by attrition grinding.

The vacuum hot pressed (VHP) billet is then skin cut by lathe and given a 870°C heat treatment and step cool to force all aluminum impurities into an

19980401 092

¹ Conducted for the United States Department of Energy under Contract DE-AC04-94AL85000

DISTRIBUTION OF THIS DOCUMENT IS UNLIMITED

MASTER

DTIC QUALITY INSPECTED 3

DISCLAIMER

This report was prepared as an account of work sponsored by an agency of the United States Government. Neither the United States Government nor any agency thereof, nor any of their employees, makes any warranty, express or implied, or assumes any legal liability or responsibility for the accuracy, completeness, or usefulness of any information, apparatus, product, or process disclosed, or represents that its use would not infringe privately owned rights. Reference herein to any specific commercial product, process, or service by trade name, trademark, manufacturer, or otherwise does not necessarily constitute or imply its endorsement, recommendation, or favoring by the United States Government or any agency thereof. The views and opinions of authors expressed herein do not necessarily state or reflect those of the United States Government or any agency thereof.

iron-aluminum-beryllium intermetallic compound (AlFeBe₄). The billets are then machined into the required shapes by conventional methods (turning, milling, EDM, drilling, etc.) using carbide tools. Machining beryllium is similar to machining heat treatable aluminum alloys. Furthermore, beryllium has a microscopic layer of damaged metal after machining. This damage affects mechanical properties, particularly ductility. Maximum mechanical properties can be recovered after machining by etching 0.08 - 0.13 mm of metal off each surface using a 2% HF - 2% HNO₃ - 2% H₂SO₄ solution. The surface then has a matte appearance and finish. If etching cannot be done or is not required, the beryllium can be machined to a 125 rms microinch surface finish and given a stress relief heat treatment to minimize the effect of machining damage on properties.

2. EXPERIMENTAL

2.1 Materials

The composition and principal impurities of Lot 4971 are shown in Table 1 below. It was from this lot of alloy that all tests were performed. These specimens were etched after machining as described in the previous section.

Table 1.
Composition of S-65C Beryllium
Lot 4971; (wt. %, except as noted)

ELEMENT	wt %
Be	99.54
BeO	0.60
C	0.012
Al	185 ppm
Fe	620 ppm
Ni	130 ppm
Si	160 ppm
Other	<100 ppm ea.

As indicated above, vacuum hot pressing of beryllium results in a material with some degree of anisotropy in mechanical properties. Strength and ductility measured parallel to the pressing direction (longitudinal) are generally less than those measured in the perpendicular (transverse) orientation. Typical room temperature mechanical properties are shown in Table 2.[2]

Table 2
Typical Room Temperature Mechanical Properties
S-65C Beryllium

ORIENTATION	YIELD (MPa)	UTS (MPa)	DUCT. (%)
Longitudinal	251	372	3.8
Transverse	251	397	6.0
Minimum	207	290	3.0

2.2 Testing

Button end tensile specimens were tested in air at 5 temperatures: 25°C, 100°C, 200°C, 300°C, 415°C and 500°C and at a constant displacement rate of 0.004 mm s⁻¹ corresponding to an initial strain rate of 1.1 x 10⁻⁴ s⁻¹. Tests were performed on a conventional electromechanical test frame configured with a split clam-shell resistance heating furnace. Strain was determined from the output of an extensometer attached directly to the test specimens. High temperature, nickel-based superalloy springs were used to fixture the extensometer to the specimen allowing for direct measurement of strain at elevated temperatures.

3. RESULTS and DISCUSSION

3.1 Mechanical properties

Tensile curves for specimens tested in the longitudinal orientation are shown in Figure 1. It is clear that strength and ductility are strong functions of test temperature. A similar series of tensile curves are shown in Figure 2 for specimens tested in the transverse orientation. Here too,

strength and ductility were significantly affected by test temperature. The temperature dependence of the yield (0.2% offset) and ultimate tensile strengths are shown in Figures 3 and 4. The room temperature strength values agree well with those shown in Table 2. There was only a small difference in elevated temperature strength for the specimens tested in the two orientations. As expected, specimens tested with the longitudinal orientation exhibit somewhat lower strength than those tested with the transverse orientation. The effect of orientation on mechanical properties diminishes with increasing test temperature.

Both orientations exhibited yield point phenomena, an example of which is shown in Figure 5 for a specimen oriented in the longitudinal direction. The inset in Figure 5 shows the detail of the yield point behavior. Depending on the test temperature, specimens tested in the transverse orientation exhibited either the same or slightly greater yield point drop than specimens tested in the longitudinal orientation under the same test conditions. The orientation and temperature dependence of the yield point behavior is summarized in Figure 6. In this Figure the "yield point factor" is defined as:

$$(\sigma_{yp} - \sigma_{pl}) / \sigma_{pl}$$

where σ_{yp} is the maximum stress at the yield point, and σ_{pl} is the minimum stress in the plateau region after yielding occurs. The transverse orientation exhibited a yield point behavior at all temperatures. The longitudinal orientation did not exhibit yield point behavior at either room temperature or at 500°C. The maximum yield point for the longitudinal orientation was seen at 300°C while for the transverse orientation, the maximum was observed at 415°C. Yield point behavior is found in metals where precipitate microstructures can initially pin dislocations. The yield point then occurs at high stress levels due to the rapid multiplication of mobile dislocations. In commercially pure beryllium, Floyd [3] concluded that the yield point effect was the result of

dislocation pinning by AlFeBe_4 precipitates. Alternatively, Stonehouse [4] found no correlation with increasing aluminum content and suggested that the effect is more likely due to the presence of FeBe_{11} .

Specimens tested at 25°C and 100°C exhibited a brittle fracture with no necking near the fracture surface. Specimens tested at the higher temperatures developed extensive localized deformation prior to fracture. For these specimens, no systematic differences in ductility were observed with respect to specimen orientation. Ductility as measured by fracture strain and reduction in area are shown in Figures 7 and 8. Both Figures show a maximum at 300°C. The S-65C grade of beryllium exhibits significantly greater ductility than the commercially pure S-200E grade tested over the same range of temperature. As reported by Henshall, et. al., [5] tensile ductility of the S-200E grade (commercial purity) peaks at approximately 30% for the transverse orientation tested at 400°C. The longitudinal orientation exhibits only about half that ductility, also peaking at 400°C.

S-65C differs from S-200E in that it is derived from a more isotropic powder, has a lower total amount of metallic impurities (including Al), has a closely controlled Fe/Al ratio, and undergoes a special heat treatment to maximize conversion of all aluminum impurities from low melting point metallic aluminum to the higher melting point intermetallic compound AlFeBe_4 . The difference in high temperature elongation is probably due to all these factors.

Henshall and coworkers have also made preliminary measurements on the S-200F beryllium grade and compared it to S-200E [6]. S-200F elongation to failure at 500°C was reported to be about 25% as compared to the S-200E values, which are about 12%. The S-200F beryllium grade is very similar to S-200E in terms of chemical composition and thermomechanical processing history. However, S-200F is made

from the more isotropic impact ground powder while S-200E is made from attrited powder. The influence of the powder type cannot be discounted. Figures 9-11 compare the present data for longitudinal orientation to other data for S-65C measured by Smith et. al [7] and Brush Wellman (B-W) production data. There is overall good agreement between the data sets. As shown in Figure 9, the present UTS data lie between the data by Smith et. al and the production data. In Figure 10 it can be seen that the present yield strength data lies below the two other data sets up to 200°C and between them after that. The percent elongation data is shown in Figure 11. The present data lies above the other two data sets up through 200°C but then comes into agreement with the other data sets at 500°C.

All of the mechanical property results described here are summarized in Table 3.

3.1 Fractography

Scanning electron microscopy was used to characterize the fracture surfaces of all of the tensile specimens. At any given temperature, the fracture surfaces of the two different orientation were quite similar in appearance. However, significant differences were noted as a function of test temperature. Specimens tested at room temperature, 100°C and 200°C all exhibited 100% cleavage fracture. Figure 12 shows the typical smooth crystallographic faceting observed for the specimens tested at room temperature and 100°C. The individual facets are well defined. At 200°C, the fracture surfaces had a somewhat different appearance as shown in Figure 13. While the fracture is still entirely cleavage, it is much flatter than that observed at the lower temperatures. Individual facets are much more difficult to define and the lines of cleavage seem to follow a much more macroscopic pattern of river lines which are more easily seen at lower magnifications (not shown).

Specimens tested at 300°C exhibited two distinct fracture morphologies. These fracture morphologies are apparent in Figure 14, a low magnification SEM image of the longitudinally oriented specimen. Approximately 50% of the fracture surface can be characterized as cleavage while the remaining half is ductile rupture and the transition between the two fracture morphologies is quite abrupt. The cleavage portion of the fracture surface is similar to that shown in Figure 13. The ductile fracture morphology is shown in Figure 15 from which it is clear that fracture has occurred via microvoid growth and coalescence. Dimple size varies from a few microns to as large as 20 microns. At very high magnifications there is no evidence of discrete nucleation sites for these voids (i.e., oxides).

At the highest test temperature, fracture was uniformly ductile in character with no evidence of any cleavage fracture. The fracture surfaces for these specimens looked similar to that shown in Figure 15 with the only difference being the presence of fewer large dimples.

REFERENCES

1. N. T. Borch, Elevated Temperature Behavior, in Beryllium Science and Technology, vol. 1., eds., D. Webster, G. J. London, Plenum Press, New York, 1979
2. D. E. Dombrowski, E. B. Deksnis, M. A. Pick, Thermomechanical Properties of Beryllium, Atomic and Plasma-Material Interaction Data for Fusion, vol. 5, ed., R. K. Janev, International Atomic Energy Agency, p. 19 - 76, Vienna, 1994
3. D. R. Floyd, Causes of the Yield Point Phenomenon in Commercial Beryllium Products, Report No. RFP-2061, Rocky Flats Div. Dow Chemical Inc., February 1974
4. A. J. Stonehouse, Impurity Effects in Be, Beryllium Science and Technology, vol. 1, eds.,

D. Webster, G. L. London, Plenum Press, New York, 1979

5. G. A Henshall, S. G. Torres and J. E. Hanafee, The Elevated Temperature Properties of S-200E Commercially Pure Beryllium, Lawrence Livermore Laboratory Report, UCRL-ID-120258, March 1, 1995

6. S. G. Torres, G. A. Henshall, J. E. Hanafee,

The Elevated Temperature Properties of S-200E Commercially Pure Beryllium, 2nd IEA for Fusion, Jackson Lake Lodge, Wyoming, September 6-8, 1995

7. M.F. Smith, R.D. Watson, J.B. Whitley, J.M. McDonald, "Thermo-mechanical Testing of Beryllium for Limiters in ISX-B and JET", Fusion Technology, vol. 8, pp. 1174-1183, July 1985

TABLE 3:
Summary of Mechanical Properties of S-65C Beryllium

	ORIENTATION	25°C	100°C	200°C	300°C	415°C	500°C
YIELD* (MPa)	Longitudinal	232	229	211	190	173	140
	Transverse	248	241	224	195	176	146
YIELD PT. Max (MPa)	Longitudinal	---	230	220	200	186	---
	Transverse	251	244	232	207	196	145
YIELD PT. Min (MPa)	Longitudinal	---	229	213	185	173	---
	Transverse	246	240	224	190	172	140
UTS (MPa)	Longitudinal	376	368	317	257	224	185
	Transverse	399	381	324	261	217	182
UNIFORM STRAIN (%)	Longitudinal	4.9	9.5	10.1	8.7	7.3	7.8
	Transverse	5.0	16.8	11.2	8.8	7.1	6.5
FRACTURE STRAIN (%)	Longitudinal	4.9	11.8	42.9	53.9	32.4	25.6
	Transverse	5.0	16.8	46.3	50.6	24.5	31.5
REDUCTION in AREA (%)	Longitudinal	5.1	10.9	48.8	71.9	57.8	48.0
	Transverse	5.1	12.3	44.2	69.1	65.0	46.3

* 0.2% Yield Strength,

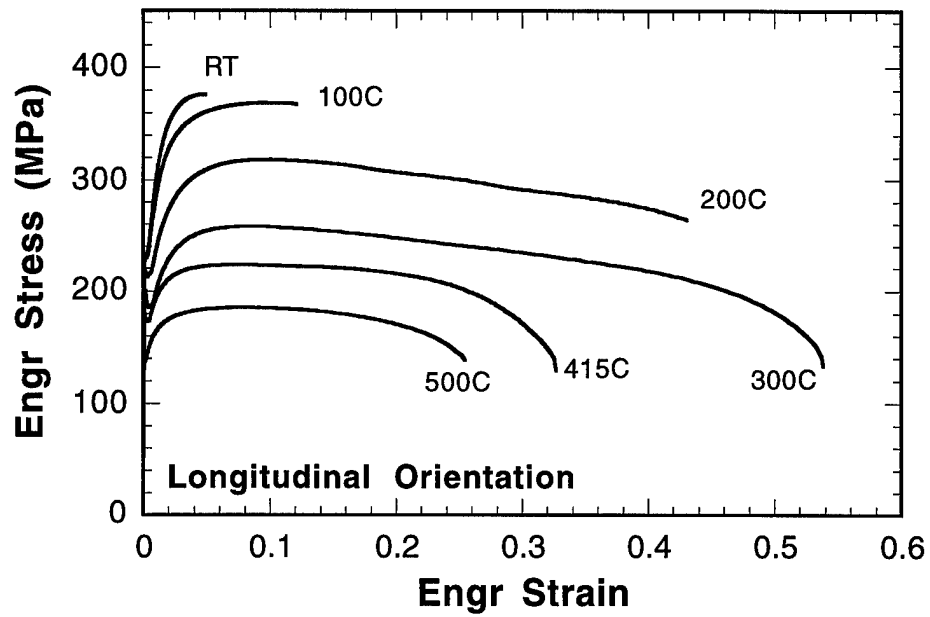


Figure 1. Stress-strain curves for specimens tested in the longitudinal orientation.

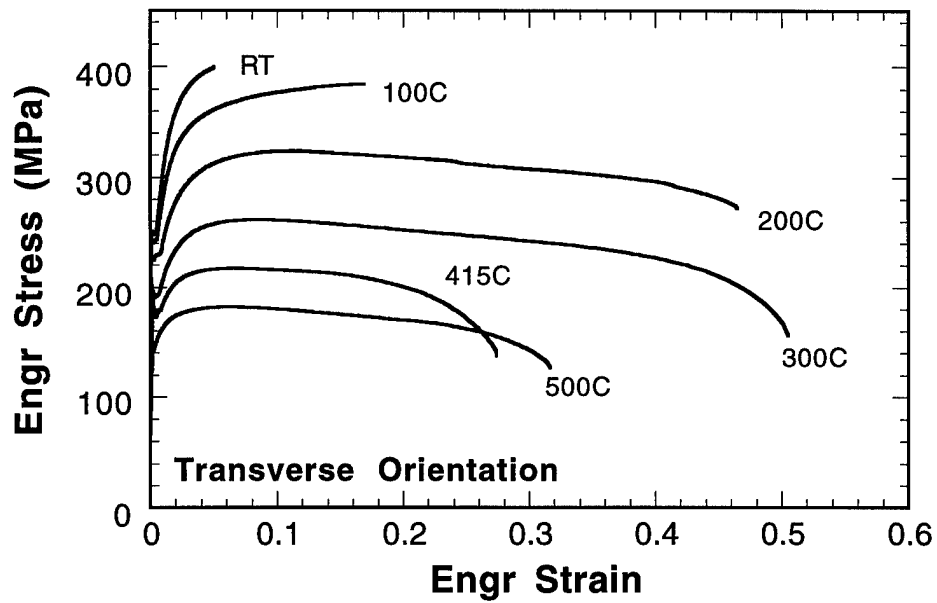


Figure 2. Stress-strain curves for specimens tested in the transverse orientation.

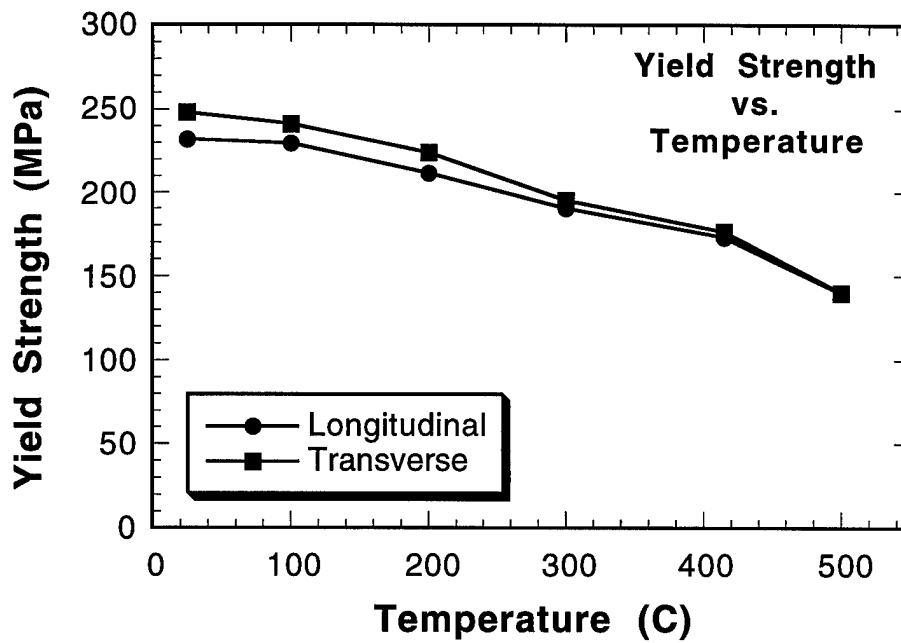


Figure 3. Yield strength decreases with increasing test temperature

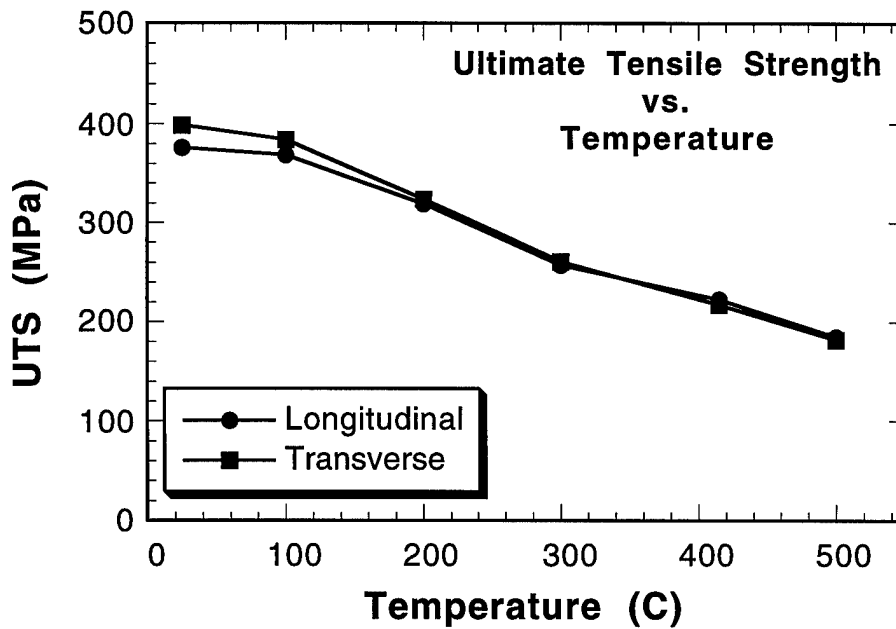


Figure 4. Ultimate tensile strength decreases with increasing test temperature

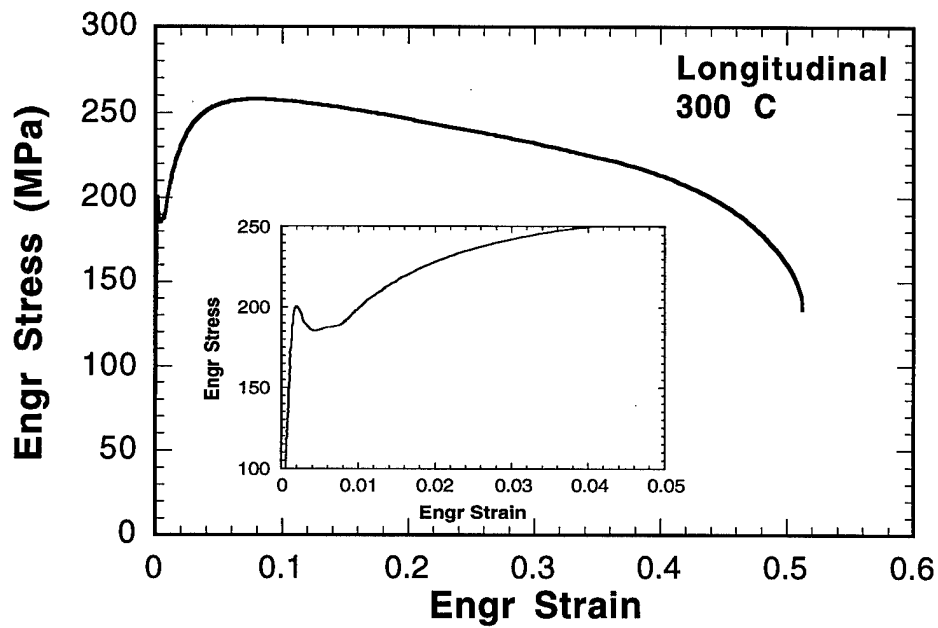


Figure 5. S65C exhibits yield point phenomenon (see inset).

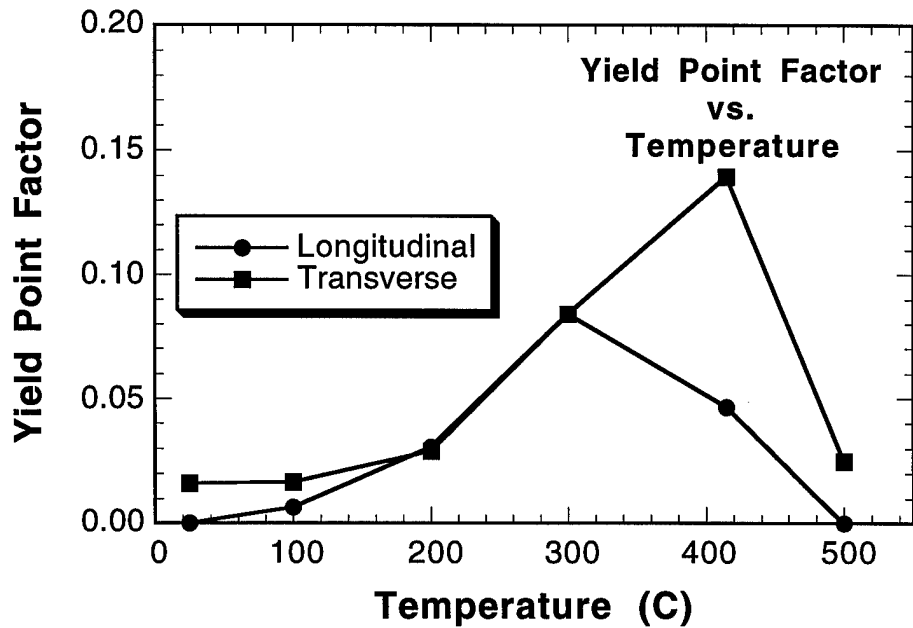


Figure 6. The magnitude of the yield point effect is dependent on test temperature.

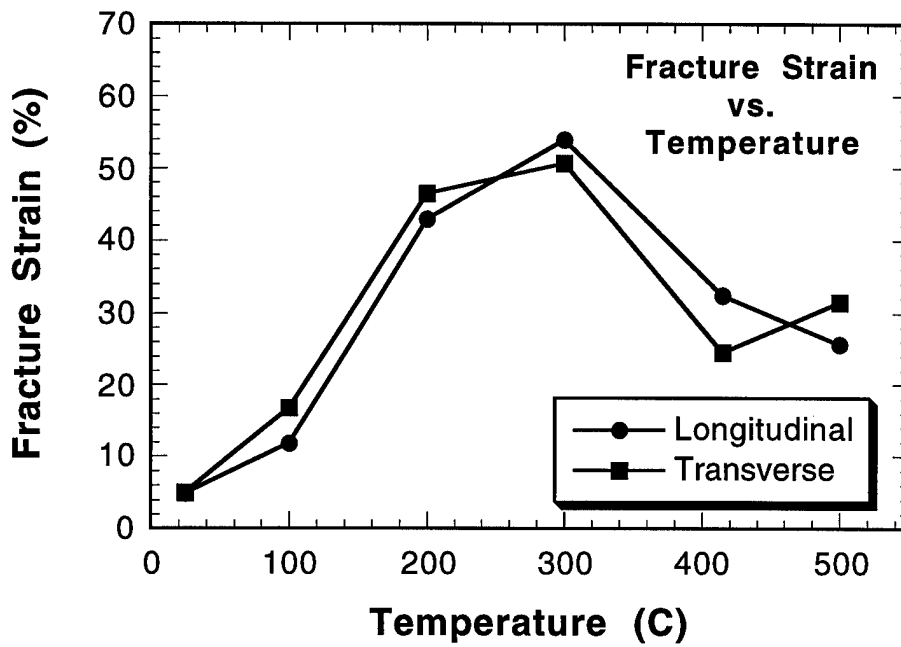


Figure 7. Ductility maximum is seen at 300°C for both orientations

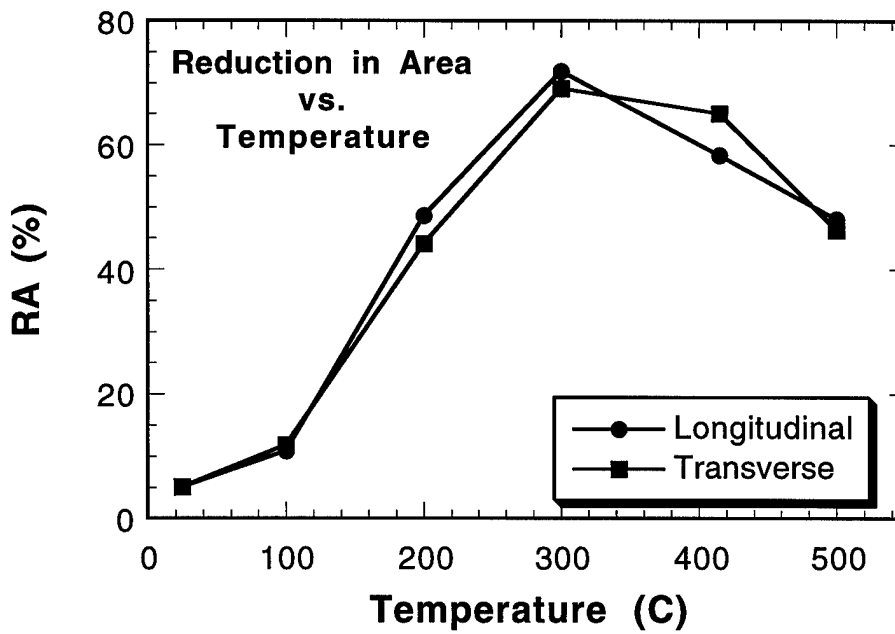


Figure 8. Reduction in area shows the same temperature dependence as the fracture strain

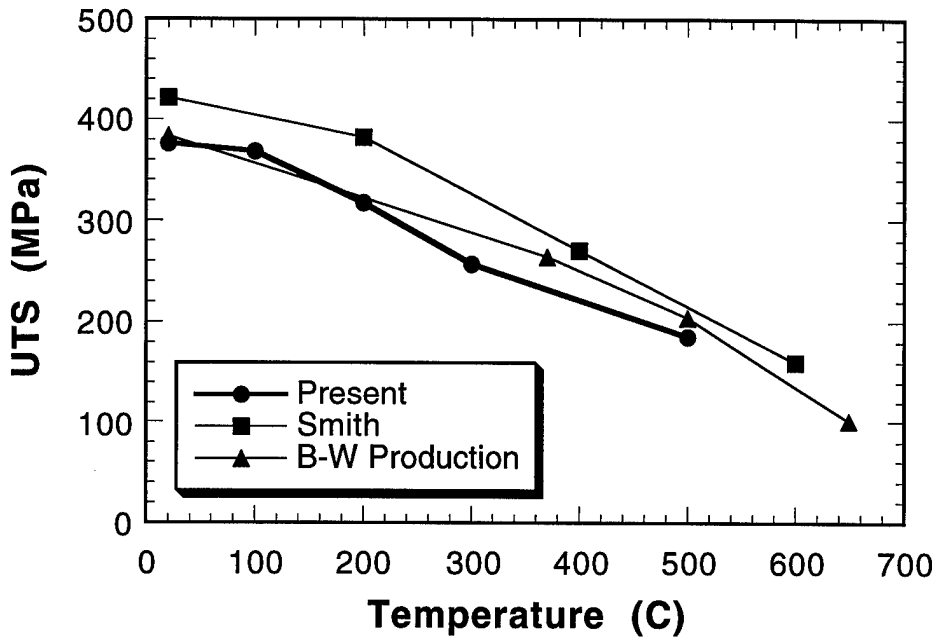


Figure 9. Comparison of present work (UTS) to previous studies

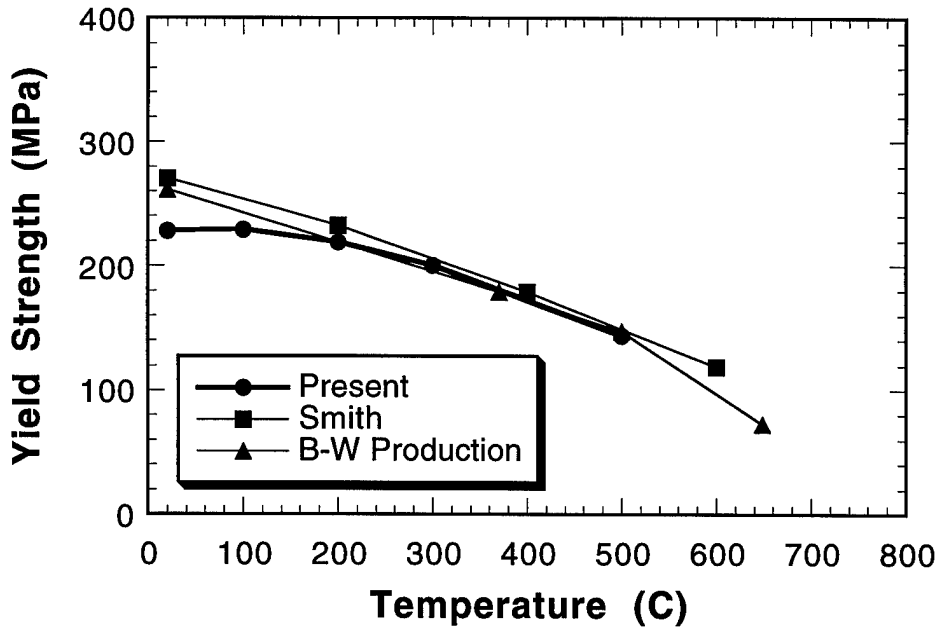


Figure 10. Comparison of present work (Yield Strength) to previous studies

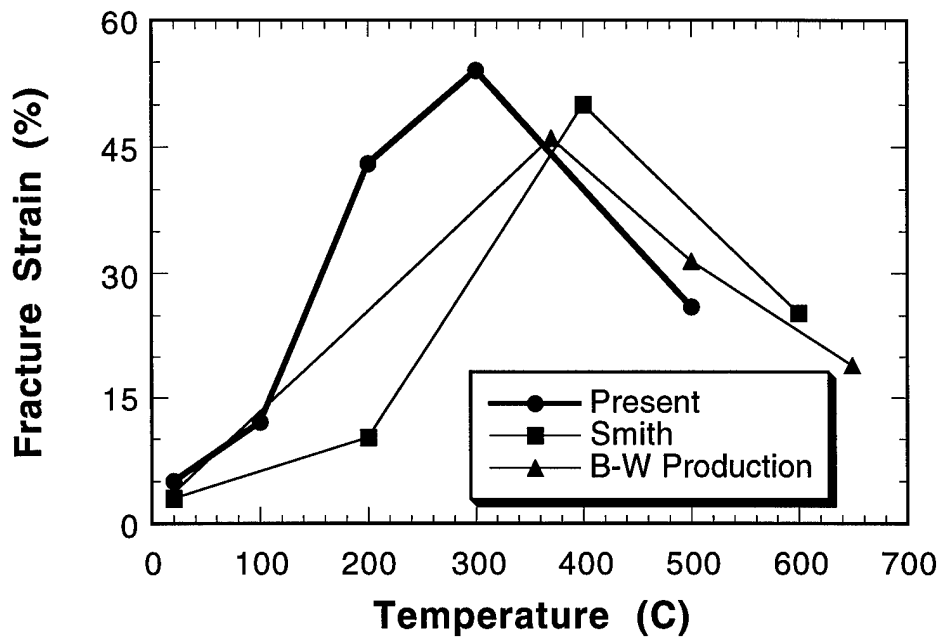


Figure 11. Comparison of present work (ductility) to previous studies.

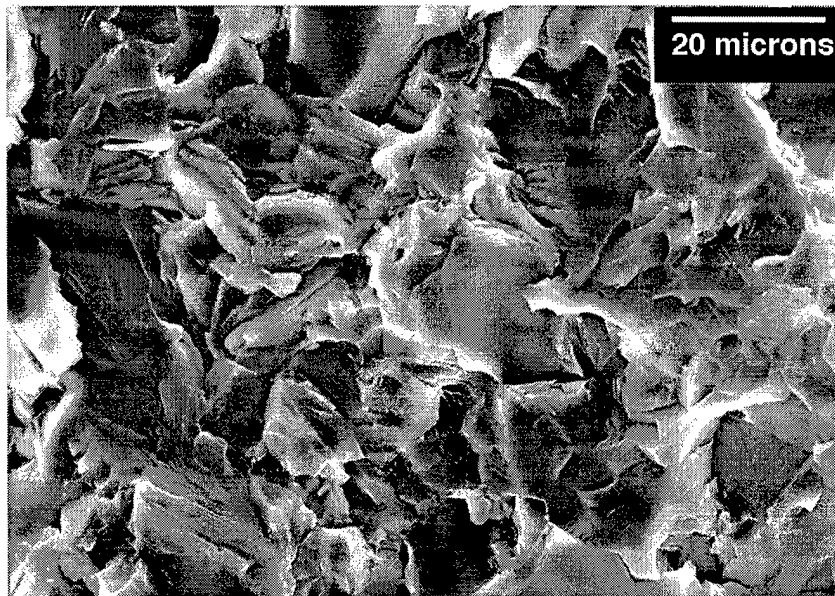


Figure 12. Fracture morphology for the specimen tested at 100°C is typical of the 100% cleavage fracture for specimens tested at this temperature and at room temperature.

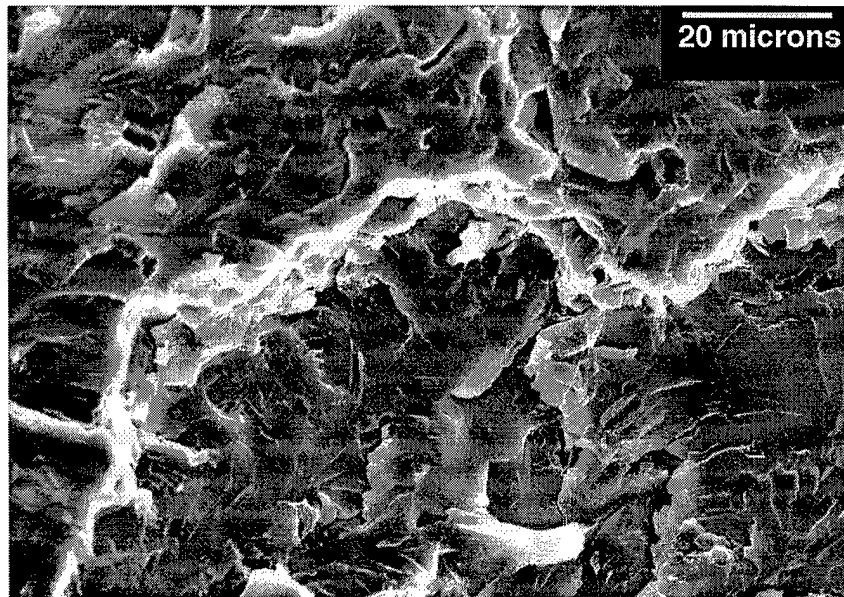


Figure 13. Cleavage fracture at 200°C is flatter than that observed at the lower temperatures. Individual facets are much more difficult to define than at the lower test temperatures. The high contrast features are part of river lines which are more easily seen at lower magnifications.

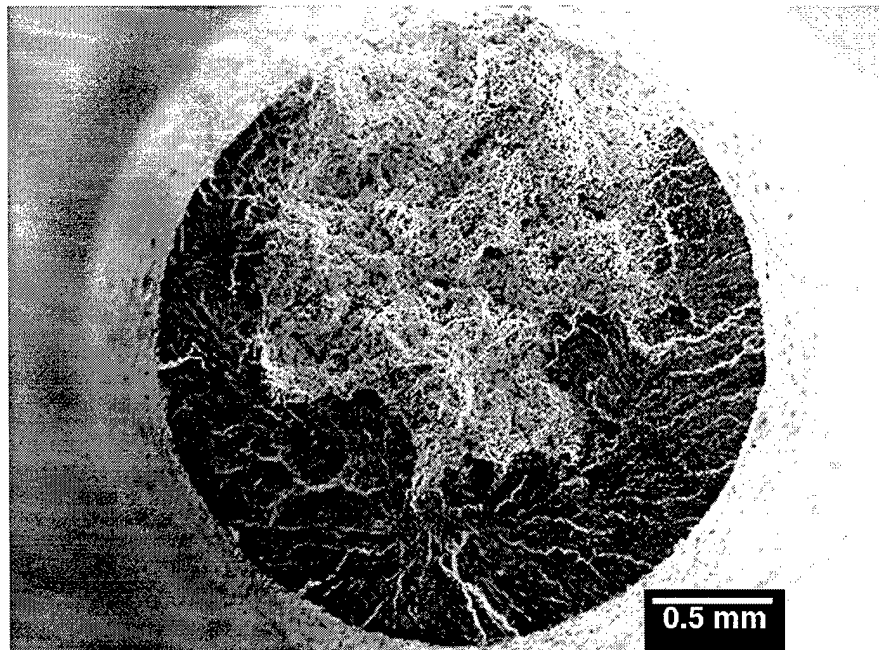


Figure 14. Fracture surfaces at 300°C exhibit nearly equal fractions for ductile and cleavage fracture.

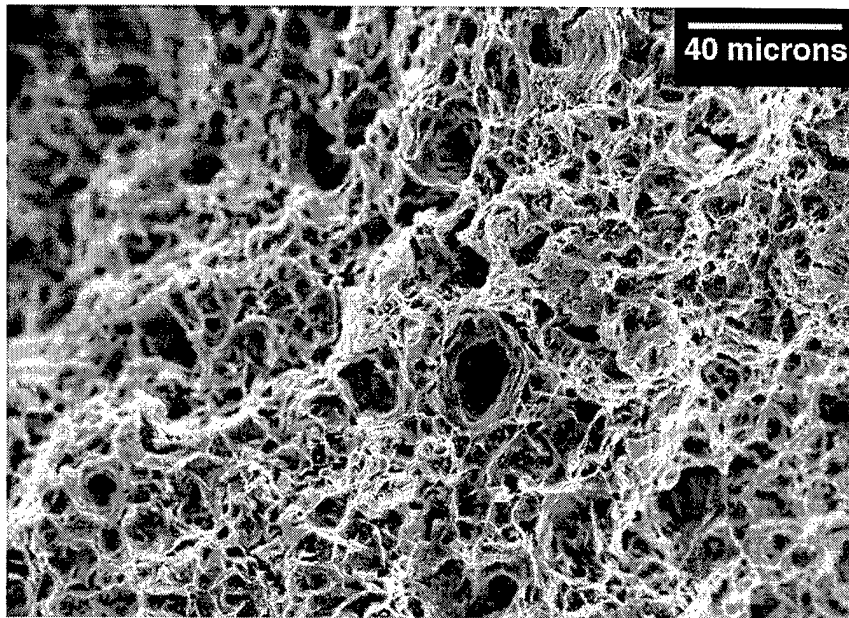


Figure 15. Ductile fracture morphology is characteristic of the central “core” of the fracture surface shown in the previous Figure.

M98050609



Report Number (14) SAND--98-8400C
CONF-9710153--

Publ. Date (11) 199711

Sponsor Code (18) DOE/ER, XF

JC Category (19) UC-400, DOE/ER

DOE